Modeling for Preliminary Stray Current Design Assessments

Modeling for Preliminary Stray Current Design Assessments: The Effect of Cross-Track Regeneration Supply

C. A. Charalambous, *Member, IEEE,* I. Cotton, *Senior Member, IEEE, P. Aylott,*

***Abstract*— Simulators of different approaches and scales have been reported in literature in an attempt to investigate the generation and impact of stray currents resulting from the operation of DC rail transit systems. Bearing in mind the existing methods for stray current modeling and control, this paper offers an important modeling advancement. A model is developed to quantitatively assess the more complex stray current picture arising from the effect of cross-track regeneration supply. Cross track regeneration refers to the case where a train in one tunnel is collecting current from a regenerating train in an adjacent tunnel, as power saving endeavour.**

***Index Terms*— DC Transit Systems, Stray Current Design and Control, Bored Tunnel Systems, Cross-Track Regeneration, Corrosion Risk.**

I. Introduction

THE elevation in rail potential caused by the flow of traction current has the ability to cause current leakage from the rails, usually described as stray current. Corrosion will occur at each point that current transfers from a metallic conductor, such as a reinforcement bar in concrete, to the electrolyte (i.e. the concrete). Hence stray current leakage can cause corrosion damage to the rails, the tunnel reinforcement and to third party systems such as external buried pipework. Severe damage may occur as a result of stray current leakage [1].

The stray current impact of any individual DC railway can be managed in a number of ways. In broad terms, the issues that impact on stray current performance can be summarised as: a) the conductivity of the traction current return circuit (i.e. the rails), b) the quality of insulation of the return circuit from earth, c) spacing of supply substations, d)train current demand, e) substation and system earthing and f) regenerative braking.

A thorough literature review reveals that the majority of the constraints listed above are well defined and understood. In particular the impact on stray current levels due to the conductivity and insulation of the return circuit is reported in [2]-[5]. Other related literature describe the influence of train current demand on the DC traction stray current perfomance, both statically and dynamically [6]-[10]. Moreover the different substation and system earthing schemes utilised in DC traction systems and their influence in their stray current performance are addressed in [11], [12].

However, it appears that there is a gap in the literature regarding simulation models that are able to quantitavely assess the stray current performance of DC traction systems under the effect of cross-track regeneration. Under this condition the stray current disitribution of the system becomes more complex.

A. Cross Track Regeneration and Stray Current Performance Evaluation

Cross track regeneration refers to the case where a train on one set of running rails is collecting current from a regenerating train on an adjacent set of running rails as a power saving endeavour. A comprehensive description of a DC-traction power system software that enables the situation, with trains operating in regenerative-braking mode, to be simulated is reported in [13].

In the context of stray current assessments for DC traction systems, the stray currents produced during regenerative braking operation are not thought to be adequately controlled. However, the effect of cross track regeneration has not been quantitatively assessed in literature. A recent work [14] merely reports that the introduction of regenerative braking has had significant (negative) impact on the capability to safely mitigate DC stray currents. This is because regenerative braking converts the DC traction locomotive into a moving power source during braking operations therefore both the source and the load move around the system making it difficult to design an effective stray current mitigation system. As a result, many stray current modeling endeavours report that the effect of regenerative braking is inevitably ignored at the early stage of stray current control design process [15], [16].

Consequently the main objective of this work is to offer a quantitative assessment of the more complex stray current picture arising from the effect of cross-track regeneration. This kind of assessment may be considered at the early stages of the design process. The models developed for this work are based on a stray current assessment for a Bored Tunnel System (B.T.S) using a commercial software platform [17]. The design options incorporated for the static models are based on

C.A. Charalambous is with the Department of Electrical and Computer Engineering of University of Cyprus, PO Box 20537, 1687, Nicosia, Cyprus (e-mail: cchara@ucy.ac.cy).
Ian Cotton is with the School of Electrical and Electronic Engineering of the University of Manchester, M60 1QD, Manchester, U.K. (e-mail: ian.cotton@manchester.ac.uk).
Pete Aylott is with Intertek- CAPCIS, M1 7DP, Manchester, U.K. (e-mail: pete.aylott@intertek.com).

realistic 3D civil drawings and on other particulars taken from a real system. Thus the global impact, of cross track regeneration on the Stray Current Collection System (S.C.C.S), the tunnel reinforcement and on a third party infrastructure, can be quantitatively assessed.

II. Description of Base Simulation Model

Fig. 1 illustrates a cross-section of a realistic B.T.S along with actual dimensions, labeling the most important features that are crucial in assessing its stray current performance.

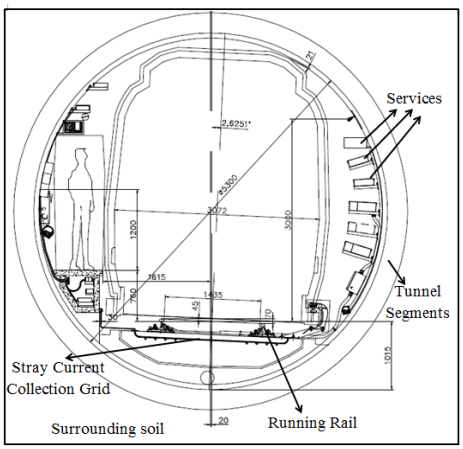

Fig. 1. Cross Section of a realistic B.T.S with actual dimensions in mm.

A. Characteristics of Base Simulation Model

An appropriate simulation model has been formulated within the MALZ module of the CDEGS software [17] to serve as a reference model (see Fig. 2).

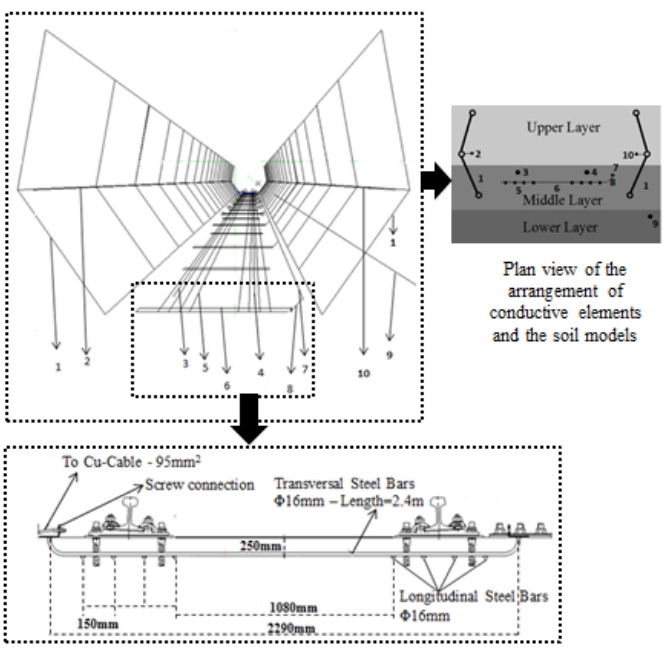

Fig. 2. Perspective view of the arrangement of conductive elements in B.T.S. model

The MALZ module allows currents to be injected and collected at various points in a network of conductors that are placed in a soil environment. It further computes the flow of these currents through each individual conductor within the network. It thus offers the advantage of computing a stray current and a voltage distribution along the length of the system modeled [18]. The design options are based on realistic 3D civil drawings and on other particulars taken from a real system as shown in Fig. 2. The model embraces the return circuit elements found in a Bored Tunnel System. These elements are formulated by 837 individual conductors subdivided in 4793 segments. Each conductor segment is given a certain material type and coating characteristics as tabulated in Table I.

TABLE I
Description of Conductive Elements

Numbered Items	Further Particulars
Tunnel Segments (Item 1)	The tunnel segments are not electrically continuous. Two segments (item 1 – left and right are considered in the model, since electrically conductive tunnel services may be attached to them. While the tunnel segments are approximately 1m in length, they are modelled as 50m segments in the computer model to restrict the overall number of conductors.
Tunnel Services (Items 2 &10)	Modelled as galvanised steel conductors. The tunnel services are modeled to represent an overall tunnel service cross-sectional area of 79 mm² (item 2), equating to a conductor radius of 5 mm and an overall tunnel service cross-sectional area of 314.16 mm² (item 10), equating to a conductor radius of 10 mm. The model allows for the tunnel services to be continuous but these are insulated from the tunnel segment reinforcement.
Running rails (Items 3 &4)	Modelled as conductors (e.g. UIC54) having a longitudinal resistance of 40 mΩ per kilometer. As it is not possible to model discrete insulator pads in the software, the effect is modeled by assuming the rails are coated with a resistive coating. This coating is set accordingly to account for a resistance to earth 100Ω.km.
Stray Current Collection Grid – Longitudinal and Transversal Steel Bars (Items 5 &6)	The S.C.C.S. consists of the Stray Current Collection Grid (S.C.C.G.) and the Stray Current Collection Cable (S.C.C.C.). The S.C.C.G. employs steel bars which are longitudinally placed (item 5) under each rail (4 steel bars x Φ16 mm for each running rail - that is 2 x 4 steel bars x Φ16 mm for a single track). This design provides an overall S.C.C.G. cross-section of 1608 mm^2 per track as is shown in Fig. 2
Stray Current Collection Copper Cable – (Items 7 & 8)	The Stray Current Collection Cable (S.C.C.C. - item 7) is bonded to the S.C.C.G. through flexible bare cables (item 8) at 100 m intervals. Both cables are made from copper and their size is taken in the model as 95 mm^2. The cables are insulated.
Third-Party Infrastructure (Item 9)	The conductor (item 9) representing the third party infrastructure serves the scope of assessing the effect of stray current on samples of the metallic infrastructure that lies in the nearby vicinity of the tunnel system. Within the model developed it takes the form of a metallic (heavy duty galvanised steel) coated conductor.

The model of Fig.2 has also incorporated into it, a three-layer horizontal soil model. For this type of soil model the potentials are computed using an analytically derived kernel [19]. This arrangement mirrors the real situation well and is computationally stable as detailed in [18]. The upper layer of the soil model is assigned an extremely high resistivity of 10^{14} Ωm, to eliminate any leakage current to flow from the rails to tunnel services in an upward direction. A portion of the tunnel segments is situated in the middle soil layer which is assigned a resistivity of 180 Ω.m. This represents the concrete present within the tunnel. The lower layer of the soil model is assumed to have a resistivity of 15 Ωm (i.e. a lowest likely measured figure) and represents the soil surrounding the tunnel. It is reiterated that from a stray current perspective the worst case should be the lowest likely measured soil resistivity figure and

recognized that under some environmental conditions this could be lower than the value used here. Table II tabulates the base input data and assumptions employed in subsequent simulations for assessing the stray current performance of the model of Fig. 2.

TABLE II
BASE INPUT DATA AND ASSUMPTIONS

Parameter (Per Tunnel/Track)	Description
Track length & power supply	1 km single track with a supply substation at either end.
Traction current	2000 A static load at 250m (motoring)
Rail resistance	40 mΩ/km (UIC54)
Rail conductance (resistance to earth)	100 Ω.km
Soil Model Resistivity /Width	Upper: 10^{14} Ω.m / 5.8m Middle: 180 Ω.m (Concrete) /1m Lower: 15 Ω.m /Infinite
Stray Current Collection Grid (S.C.C.G.)	2 x 4 steel bars x Φ16 mm for a single track
Stray Current Collector Cable (S.C.C.C)	95 mm^2 - copper – bonded to S.C.C.G. at 100m intervals
Stray current collector cable termination at substations	Floating
Tunnel Depth	6m below ground level
Tunnel Reinforcement	Φ20 mm- Steel (Tunnel segments electrically isolated along the length of tunnel)
Tunnel Services	79 mm^2 (left) / 314.16 mm^2(right) - galvanised steel
Insulation of internal tunnel infrastructure (handrail, fire main etc.) from segment reinforcement	insulated connection to tunnel reinforcement: 1MΩ
Third Party Infrastructure	1963 mm^2 - galvanised steel

B. Description of Energisation Model –Base Scenario

The simulation model can assess the impact of a single point load at discrete locations with traction supply substations at each end. The model is also able to capture the floating nature of the system and can assess various topological design options of the Bored Tunnel Systems (B.T.S.).

The base model assumes two cases as shown in Fig. 3. The first scenario assumes that the train is placed 500m from the origin of the track (*A*), while the second scenario simulates the train at 250m from the origin of the track (*B*). In both cases, the train is modeled as a motoring load (i.e. drawing 2000 A current from the two substations located at either end of the track).

It is noted that the simulated case *A* (i.e. symmetrical 1 km section of tunnel with a single train at the center and a substation at each end) represents the worst static case scenario in terms of stray current performance evaluation.

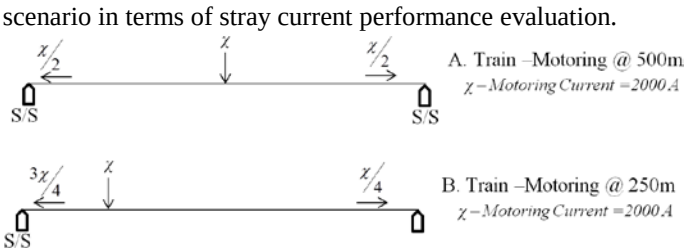

Fig. 3. Base Model: One B.T.S with a Motoring Train at different Locations (Scenario *A* at 500m – Scenario *B* at 250m)

C. Simulation Results and Analysis

The simulations are carried out using the 1 km sections of the tunnel system illustrated by Fig. 2. The simulation takes about 2.5 hours to be completed on a standard computer (2GHz processor, 3GB RAM). Fig. 4 illustrates the simulated rail to earth voltage (for $Rail_1$ –item 3) simulated by the F.E model of Fig. 2 for the two scenarios presented in Fig. 3. It can be shown that the same profile is obtained for $Rail_2$ (item 4) in each scenario. The current returns to the supply substations via the running rails; in a proportion determined by the relative location of the train with respect to its feeding substations. This produces a rise in the rail to earth potential which in turn results in stray currents in a proportion determined by the relative location of the train. In a floating rail system, the stray currents are determined by the combination of the rail potential and the resistance of the trackwork insulators.

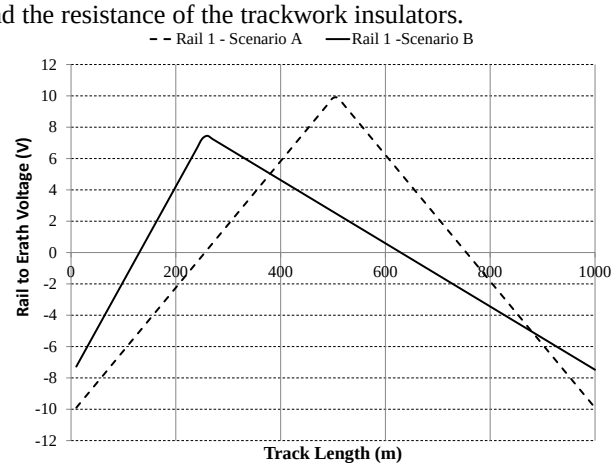

Fig. 4 Simulated Track to Earth Voltage – Base Model

A rough calculation of the expected stray current for scenario *A* can be made by hand. Take 2000 A equally returning through a section of 500m of two rails (i.e. 1000 A on each side) with a resistance of 40 mΩ/km of rail. Since the two rails are in parallel, the overall potential difference between the midpoint and rail ends will be 20 V. In the convention of this modeling, this will appear on the rails as +10V to remote earth near the train and –10V to remote earth near the two substations. A positive voltage implies a current leaking out of a conductor by corrosion; a negative voltage implies a current leaking into a conductor. At 250 m down the track the voltage to remote earth will be 0 V. The running rail is taken to have a resistance to earth of 100 Ωkm. The resistance to earth of 250 m of running rail is therefore 400Ω. The total stray current leaving the running rail will therefore be given by 5 V (the average running rail voltage along a 250 m length) divided by 400Ω, in other words 12.5 mA. The total stray current will therefore be approximately four time this, 50 mA, since there are two running rails in either of the 500 m sections which each allow current to leak to earth. A similar calculation can be shown for scenario *B*. Besides hand calculations, the results of Fig. 4 have been extensively verified by the classical resistive type approach that is widely used in the literature [9], [20]. Furthermore the software employed in this study, has itself been shown to be accurate by many researchers across the world and has been extensively verified. The models used in this paper are simplifications of a real system but these simplifications were used after confirming that they did not cause an error in any expected current/voltage of more than 1% [24].

Fig. 5 illustrates the simulated geometrically accurate 3D plot of the net leakage current profile of the two Stray Current

Collection Grids (S.C.C.G) when the train is located at 250m from the origin (i.e. scenario *B*).

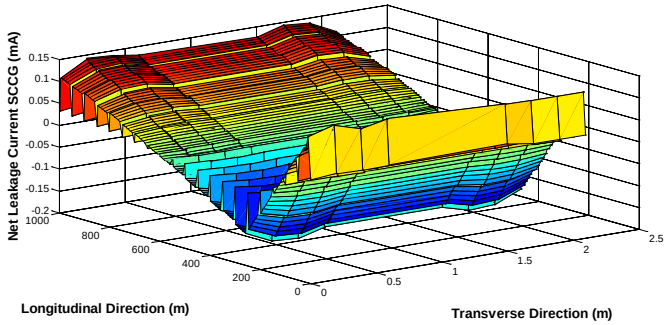

Fig. 5. Simulated Net Leakage Current S.C.C.G – Base Model – Scenario *B*

Fig. 6 illustrates the simulated geometrically accurate 3D plot of the current retained by the S.C.C.G, while Fig. 7 the corresponding track to earth voltage profile.

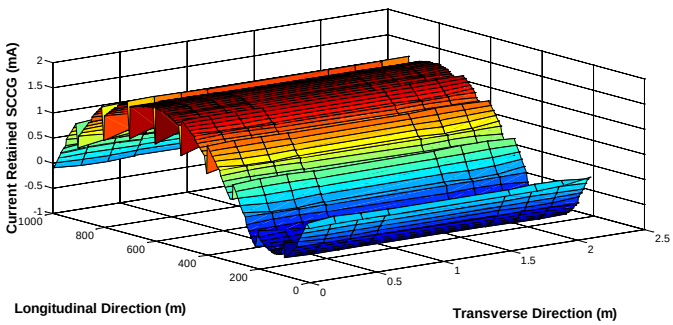

Fig. 6 Simulated Retained Current S.C.C.G – Base Model

Table III illustrates the summary of the stray current generation and its consequent allocation simulated for the model of Fig.2. It is noted at this point that the percentage of current flowing in the S.C.C.S (S.C.C.G +S.C.C.C), i.e. its efficiency, can be assessed at a point where the net leakage current of the S.C.C.S is zero (see Fig. 5) and the collected current by the S.C.C.S conductor elements is at an absolute maximum (see Fig. 6). By representing the total stray current flowing from the running rails as a percentage of the stray current collected by the grid, the efficiency of the S.C.C.S can be determined. The remainder of the stray current will flow through unintended paths (e.g. earth).

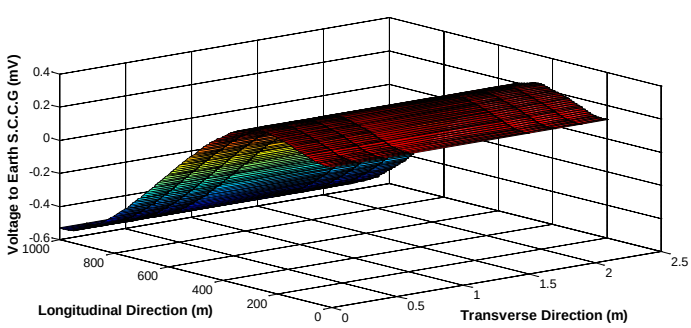

Fig. 7. Simulated Track to Earth Voltage S.C.C.G – Base Model

Table III also illustrates that the total stray current calculated from the model (50.171 mA) coincides with the hand calculations (50 mA) presented earlier (Scenario *A* –Fig. 3). As far as the total generated current is concerned, the design engineers should note that a variation in track current will influence the leakage current distribution due to the resulting alteration of rail-to-earth potential. A doubling in track current or a doubling in substation spacing (i.e. 2km) will lead to a doubling in voltage and hence a resulting doubling of leakage current density along the rail. This is a linear effect.

TABLE III
SUMMARY OF RESULTS – BASE MODEL

Description	Scenario *A* Current (mA)	Scenario *B* Current (mA)
Total Stray Current Rails	50.171	37.604
Retained Current S.C.C.G.	24.983	18.328
Retained Current S.C.C.C.	17.495	12.634
Total Stray Current Tunnel Reinforcement	0.47081	0.40238
Total Stray Current Tunnel Services	0.00	0.00
Retained Current Tunnel Services	0.00	0.00
Retained Current 3rd party Infrastructure	0.2071	0.102
Efficiency of S.C.C.S	84.67 %	82.34 %
Current through unintended paths	15.33 %	17.66 %

Moreover, no current is collected by the tunnel services as these are modelled as being insulated from the tunnel reinforcement (see Table I). Finally, Fig. 8 illustrates the calculated voltage on a longitudinal axis parallel to the tunnel reinforcement (where *item 2* is attached – See Fig. 2).

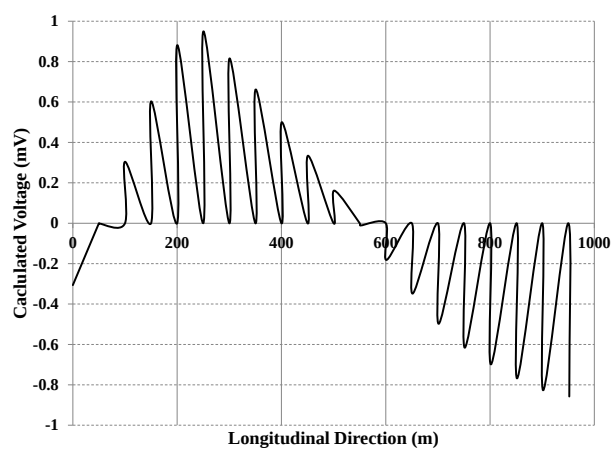

Fig. 8 Calculated Voltages on a Longitudinal Axis of Tunnel Reinforcement

It should be noted that Fig. 8 illustrates a snapshot of the simulated voltage along the specified axis. The discontinuous voltage profile confirms that the tunnel segments are electrically not continuous i.e. the reinforcement in adjoining segments (both circumferential and longitudinal) are not in direct electrical contact as segments may be bolted together through PVC sleeves. This calculation may also be used as a preliminary evaluation to check whether the maximum allowable potential value - dictated by EN 50122-2 [21] for the longitudinal voltage drop caused by operation in the tunnel is not exceeded.

III. DESCRIPTION OF CROSS-TRACK REGENERATION MODEL

The developed cross-track regeneration model is based on realistic fundamental principles of track regeneration techniques. These techniques are thoroughly described in [22] and have been integrated in a scenario where a motoring train in one tunnel is collecting current, via cross tunnel bonding of the 3rd rail supply conductor at substation and station locations, from a regenerating train in a second tunnel. It is beyond the scope of this paper to expand on the dynamics of regenerative braking in traction systems. It is reiterated that the main scope of the developed model is to quantitatively assess the more

complex stray current picture arising from cross track regeneration in the circumstance where rectifiers are used to supply two tracks i.e. trains in neighbouring B.T.Ss.

A. Characteristics of Cross-Track Regeneration Model

Fig. 9 illustrates the 3D geometrically accurate simulation model formulated to assess a cross-track power (current) transfer from a regenerating to a motoring train. The same characteristics and data input assumptions tabulated in Tables I and II hold for the model of Fig. 9 as well. It is noted that both B.T.S (A & B) have the same design characteristics both in terms of their topological arrangement and values and are separated by a distance of 15m.

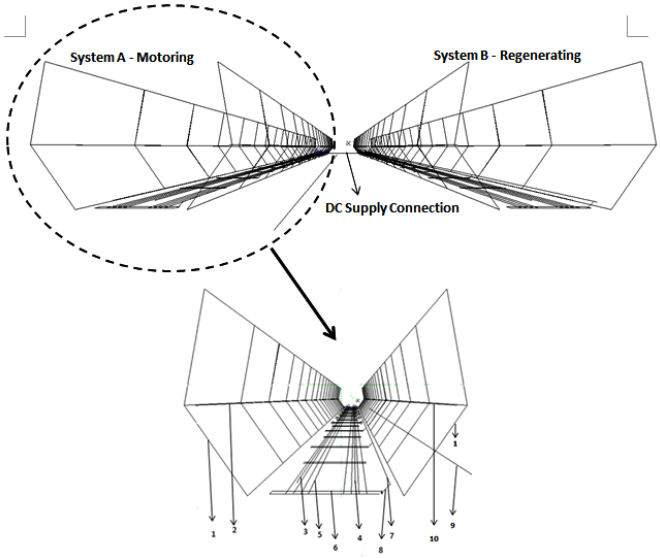

Fig. 9. Perspective view of the arrangement of conductive elements for the cross-track regeneration model (System A – Motoring at 250m, System B – Regenerating at 750m)

The trains are placed 250m from the origin of either track, i.e. there is a total train-train separation of 500m. The train in system A (250m) is modeled as a motoring load as in the base model Scenario B of Section I, whereas the train in system B (750m) is modeled as a generating load.

A DC supply connection is modeled at the location of the motoring load (at 250m). This supply connection is entitled to transfer current from the regenerating track. The connection is obviously necessary to transfer the power from one train to the other, accounting for a regeneration scenario. This is however an artificial component of the model [17] and not a direct representation of the 3rd rail conductor circuits. It is based on current sources/ sinks and cables modeled in such a way to represent a supply connection between the two tunnels (See Fig. 10).

The simulation takes about 5 hours to be completed on a standard computer (2GHz processor, 3GB RAM).

B. Description of Energisation Model (Cross-Track Regeneration)

Fig. 10 illustrates the fundamental principles of a cross-track energisation scenario. It specifically suggests that half of the regenerated current from the train in track B (i.e. $\psi/2$=1000A) is fed to that in track A at the location of the motoring load. Therefore the motoring load is powered on a 50-50 % scenario (i.e. from both systems). That is (a) by drawing current from the rectifiers that supply track A (i.e. χ-$\psi/2$=1000 A) and (b) by drawing current from the regenerating track B ($\psi/2$=1000 A). Thus a total of 2000 A (χ) is provided to the motoring load, as is the case with the scenario *B* of the base model described in Section II.

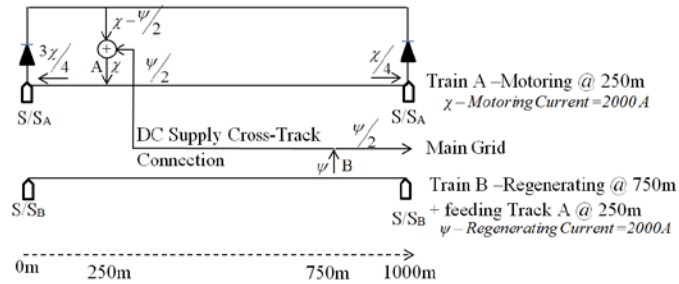

Fig. 10. Cross-Track Regeneration Scenario: Track A –Motoring, Track B, Regenerating (50-50 Scenario).

The modeled scenario aims to capture the case where some of the energy produced by the regenerating vehicles is used to partially supply the motoring vehicles in an adjacent tunnel. It should be noted that if the net energy produced by regenerating vehicles exceeds that used by motoring vehicles, the excess energy cannot be returned to the AC supply due to the unidirectional nature of the rectifiers (i.e. non-receptive supply), unless appropriate control/rectifying actions are enforced; to feed the excess energy into the main power grid [22]. Therefore the modelled scenario assumes that some regenerated power is allowed to return to the main grid supply.

C. Simulation Results and Analysis

The simulation results reflect on the effect of cross track regeneration supply on the motoring track A. The same effect and results are expected when the conditions are reversed (i.e. to examine the effect of cross track regeneration supply on track B should this become motoring). These results are benchmarked against the stray current performance of the motoring system of the base case scenario presented in Section II. This is because in both scenarios the motoring loads are supplied with a total of 2000 A, thus facilitating a sound comparison. Fig. 11 illustrates a comparison of the rail to earth voltage obtained for the motoring system of the base scenario (Section II) against the track voltage profile obtained under the cross-track regeneration (50-50) scenario.

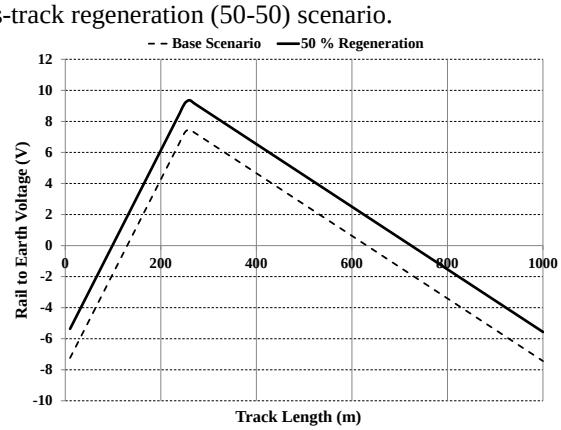

Fig. 11 Simulated Tracks to Earth Voltage – Base Scenario vs. 50-50 Regeneration Scenario

It is evident that the rail to earth potential is positively shifted by 1.875V (although the voltage difference between the

minimum and maximum voltage limits is maintained at 14 V for both cases) when the motoring load is supplied on a 50-50% scenario (i.e. 50% regeneration current from an adjacent system and 50% from its own tunnel rectifier substations). This positive voltage shift will inevitably impact on the level of the generated stray current, since the length of the track at positive potential is increased.

Table IV illustrates the summary of the stray current generation and allocation obtained for the simulation model of Fig.8, and benchmarks these against the results obtained for the base case scenario (see Table III). The results confirm that cross-track regeneration may act in reducing the efficiency of a stray current control system. More specifically, the total generated stray current has increased by 55.86 % in the cross-track regeneration scenario. That comes despite the fact that the motoring load in track A is drawing the same current in both case scenarios (i.e. 2000 A). This is due to the positive voltage shift that the floating motoring track A experiences, as a result of being partially energized from the adjacent regenerating tunnel system.

Most importantly the ability of the S.C.C.S of the System A to collect the generated stray current is decreased by 26.59 %. It should be noted at this point, that the efficiency of the S.C.C.S is associated with the number, size and placement of the constituent steel bars, with respect to the running rails. A further element that contributes to the efficiency of the system is the size of the stray current collection Cu cable (S.C.C.C). The results obtained suggest that the efficiency of the S.C.C.S can be compromised under cross-track regeneration scenarios. This should be kept in mind during any preliminary assessments that are performed to substantiate the design specification as well as the geometric topology of the collection system.

Moreover the simulated results have indicated that is likely to experience a higher stray current flow towards the third-party infrastructure that lies in the nearby vicinity of the B.T.S. In this particular example the third party infrastructure increases its retained current by 24.44 % (0.033 mA). This comes as a result of the increased stray current levels under the cross track regeneration scenario modeled.

TABLE IV
SUMMARY OF RESULTS - COMPARATIVE ASSESSMENT

Description	Tunnel Current (mA) Fig. 2	Tunnel A Current (mA) Fig. 9
Total Stray Current Rails	37.604	58.99
Retained Current S.C.C.G.	18.328	19.647
Retained Current S.C.C.C.	12.634	13.237
Total Stray Current Tunnel Reinforcement	0.40238	1.043
Total Stray Current Tunnel Services	0.00	0.00
Retained Current Tunnel Services	0.00	0.00
Retained Current 3rd party Infrastructure	0.102	0.135
Efficiency of S.C.C.S	82.34 %	55.748 %
Current through unintended paths	17.66 %	44.25 %
Description	**% Change**	
Total Stray Current Rails	55.86	
Retained Current S.C.C.G.	7.09	
Retained Current S.C.C.C.	5.50	
Total Stray Current Tunnel Reinforcement	61.42	
Total Stray Current Tunnel Services	0	
Retained Current Tunnel Services	0	
Retained Current 3rd party Infrastructure	24.44%	
Efficiency of S.C.C.S	-26.59 %	

Finally, Fig 12 compares the calculated voltage on a longitudinal axis parallel to the tunnel reinforcement for the two case scenarios (cross track regeneration scenario and base scenario - See Fig. 8).

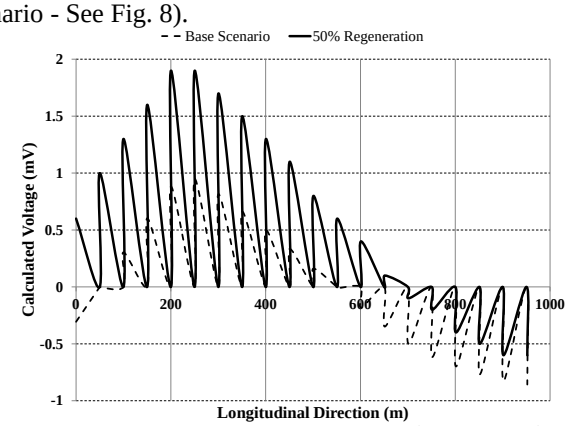

Fig. 12 Calculated Voltages on a Longitudinal Axis of Tunnel Reinforcement –Base Scenario vs. 50-50 Regeneration Scenario

A maximum potential shift of 1mV is calculated for the tunnel reinforcement under the cross track regeneration scenario. The calculated results could be correlated to the notes of EN 50122-2. These notes suggest that the acceptance criteria for successful control for the tunnel reinforcement potential shift are subject to a maximum limit of +0.2V (EN50162:2004 Table 1 [23]) which EN 51022-2:2010 interprets as 'the average value in the hour of highest traffic' although it should be borne in mind that the standard allows for significantly lower rail to earth resistance than that modeled here. It is noted that in a practical system, monitoring this voltage value, allows quantification of the stray current magnitude and direction (at the measurement location) and confirm whether a metro system is exporting and importing traction stray current through reinforced structures to and from the outside environment. This, both quantifies the corrosion threat to the tunnel reinforcement and the risk of stray current corrosion to external pipes and services.

Therefore, the evaluation of the design process followed in this study has shown the means to take into account the following inputs: a) the traction power, b) the stray current control designs as well as the distribution of the different tunnel and station construction across the system, c) significant interfaces with third-party systems and services and d) cross-track regeneration scenarios.

D. Sensitivity Analysis

A further set of simulations have been carried out to assess the influence of increasing the percentage of regeneration current that is used to energise motoring system A.

Table V tabulates a comparison of the results obtained under the 50-50 energisation scenario, a 25-75 energisation and a 0-100 energisation scenario. The 25-75 scenario reflects the case where the motoring load A is drawing 500 A current from the rectifiers that supply track A and in addition drawing 1500 A current from the regenerating track B. Thus a total of 2000 A is supplied to the motoring load, as is the case with the base scenario. The 0-100 energisation scenario reflects the case where the motoring load A draws all its current from the regenerating track B. The latter case study assumes that the

two tracks and power supply rails are interconnected at both ends (i.e. at substations locations). The simulated results under the 0-100 scenario advocate that the impact on the proposed stray current control system will be more negatively pronounced. Table V also details that the efficiency of the S.C.C.S is considerably decreased when benchmarked against the efficiency obtained for the base scenario. Moreover the negative impact on the third party infrastructure is more pronounced under the 0-100 energisation scenario.

TABLE V
COMPARISON UNDER DIFFERENT ENERGISATION SCENARIOS

	Energisation Scenario			
Description	**Base**	**50-50**	**25-75**	**0-100**
Total Stray Current Rails	37.60 mA	58.99 mA	76.58 mA	150.87 mA
Retained Current S.C.C.G.	18.33 mA	19.65 mA	20.15 mA	19.23 mA
Retained Current S.C.C.C.	12.63 mA	13.24 mA	13.47 mA	12.57 mA
Total Stray Current Tunnel Services	0.00 mA	0.00 mA	0.00 mA	0.00 mA
Retained Current Tunnel Services	0.00 mA	0.00 mA	0.00 mA	0.00 mA
Retained Current 3rd party Infrastructure	0.102 mA	0.135 mA	0.160 mA	0.368 mA
Efficiency of S.C.C.S	82.34 %	55.748 %	43.90 %	21.08%
Current through unintended paths	17.66 %	44.25 %	56.1 %	78.92 %

On a final note, Fig 13 provides the means to interpret the tabulated results of Table V. It is shown that the leakage stray current density profiles are altered for each scenario modeled although the train is supplied by the same load current (i.e. 2000A). A positive stray current density in Fig. 12 represents the case where a current leaks out of the rails into the environment. For the negative stray current density case, the current leaks back to the rails. Therefore, the simulated stray current profile of the 0-100 energisation scenario suggests that more corrosive stray current is to leave the rails since the rail region with a positive current density is increased when compared to the other cases modeled. The magnitude of the current leaking from the rails is determined by the voltage to remote earth at any point along the track and the resistance to remote earth of each rail.

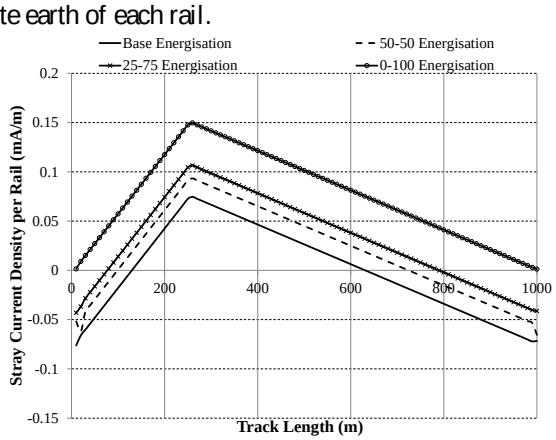

Fig. 13 Comparison of Stray Current Densities per Rail under Different Scenarios

E. Proposed Mitigation Measures

Cross bonding the rails/ tracks might be one option for the design engineers to reduce the stray current generation and its subsequent distribution as reported in [9]. Since two separate tunnel systems are considered, an alternative mitigation method is shown in the simulation model of Fig. 14. This model assumes cross-bonding of the stray current collection systems, under cross-track regeneration scenarios. Fig. 14 illustrates that the stray current collection cables (S.C.C.C) of each tunnel are linked by two conductors, one at either end of the tunnel. It is noted that the model assumes the (0-100) energisation scenario.

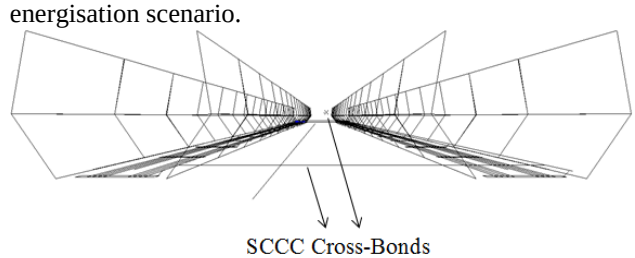

Fig. 14. Perspective view of the arrangement of conductive elements for the cross-track regeneration model (System A – Motoring at 250m, System B – Regenerating at 750m) assuming S.C.C.C cross-bonding at either end of the tunnels.

Table VI summarises the results obtained for the model of Fig. 14 and benchmarks these against the 0-100 energisation scenario results (see Table V) where no SCCC cross bonds are considered. That is to facilitate a valid comparison. Therefore, under the design inputs assumed (see Table II), the total stray current collected by the Stray Current Collection System (S.C.C.G + S.C.C.C), when S.C.C.C cross-bonding is assumed, increases by 53.07 %. Consequently less stray current flows through unintended paths to reach any third party infrastructure in the nearby vicinity. In this particular model the current collected by the 3rd party infrastructure is decreased to 0.134 mA (i.e. 63.58% reduction).

TABLE VI
COMPARISON UNDER S.C.C.C. CROSS-BONDING

Description	**No SCCC Cross Bonding Fig. 9**	**SCCC Cross Bonding Fig. 14**
Total Stray Current Rails	150.87 mA	150.96 mA
Retained Current S.C.C.G.	19.23 mA	59.32 mA
Retained Current S.C.C.C.	12.57 mA	52.62 mA
Total Stray Current Tunnel Services	0.00 mA	0.00 mA
Retained Current Tunnel Services	0.00 mA	0.00 mA
Retained Current 3rd party Infrastructure	0.368 mA	0.134 mA
Efficiency of S.C.C.S	21.08%	74.15 %
Current through unintended paths	78.92 %	25.85 %

Figure 15 illustrates the effect of introducing SCCC cross bonds at more frequent intervals along the tunnel length.

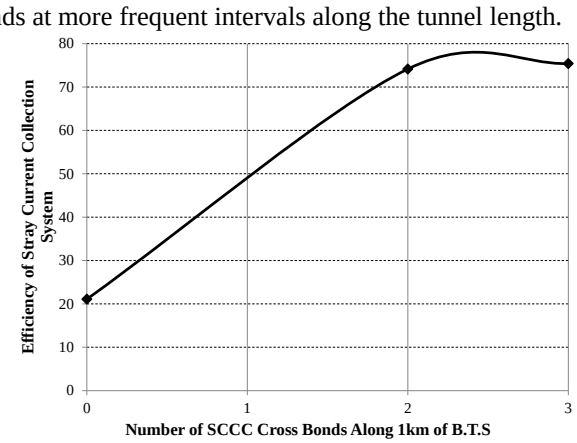

Fig. 15. Efficiency Variation of Stray Current Collection System when SCCC cross bonds are introduced along the 1km BTS modeled.

It shows the impact on the efficiency of the stray current collection system when: a) no cross bonds are introduced, b) two cross bonds (0 -1000 m) are introduced and c) three cross bonds are present (0-500-1000m). The results obtained suggest that under cross track regeneration scenarios, tunnel to tunnel cross-bonding (through S.C.C.C) could be a valuable tool to reinstate the benefits of a stray current collection system. An important conclusion is that the use of two cross bonds at either ends of the system will suffice. The use of more SCCC cross bonds will not significantly improve the efficiency of the collection system.

IV. Conclusions

This paper describes a first attempt to model and quantify the effect of cross-track regeneration on the stray current performance of a DC transit system. The cases modeled probably represent a worst case scenario but do demonstrate that regenerative braking acts to partially defeat the benefits of the stray current control system. This is unavoidable and can be minimized by maintenance of a high rail to earth resistance or by frequent tunnel to tunnel cross-bonding. Finally the effect of regenerative braking should be kept in mind during any preliminary assessments that are performed to substantiate the design specification as well as the geometric topology of a stray current collection system.

V. References

[1] Aylott, P.J.;, "Stray current is for life-not just for Christmas. Stray current corrosion management strategies for DC traction systems," DC Traction Stray Current Control - Offer a Stray a Good Ohm? (Ref. No. 1999/212), IEE Seminar on, 21 Oct. 1999, pp.7/1-7/6.

[2] Case, S.; So what's the problem? [DC traction stray current control], DC Traction Stray Current Control - Offer a Stray a Good Ohm? (Ref. No. 1999/212), IEE Seminar on, 21 Oct. 1999, Pages: 1/1 - 1/6.

[3] Ardizzon, L.; Pinato, P.; Zaninelli, D.; "Electric traction and electrolytic corrosion: a software tool for stray currents calculation", Transmission and Distribution Conference and Exposition, 2003 IEEE PES, Volume: 2, 7-12 Sept. 2003, Pages: 550 - 555.

[4] I. Cotton, C. Charalambous, P. Ernst, P. Aylott, ‘‘*Stray Current Control in DC Mass Transit Systems’’*, IEEE Transactions on Vehicular Technology, Vol. 54, No. 2, pages: 722 – 730, March 2005.

[5] Yu, J.G.; Goodman, C.J.; Modelling of rail potential rise and leakage current in DC rail transit systems, Stray Current Effects of DC Railways and Tramways, IEE Colloquium on, 11 Oct 1990, Pages: 2/2/1 - 2/2/6.

[6] Pham, K.D.; Thomas, R.S.; Stinger, W.E.; ‘’Analysis of stray current, track-to-earth potentials and substation negative grounding in DC traction electrification system’’ Railroad Conference, 2001. Proceedings of the 2001 IEEE/ASME Joint, 17-19 April 2001 ,Pages:141 – 160.

[7] Lee C. -H.; Evaluation of the Maximum Potential Rise in Taipei Rail Transit Systems, IEEE Transactions on Power Delivery: Accepted for future publication, Volume: PP, Issue: 99, 2004, Pages: 1 – 6.

[8] Bih-Yuan Ku; Hsu, T.; Computation and validation of rail-to-earth potential for diode-grounded DC traction system at Taipei Rapid Transit

[9] C. A. Charalambous, I. Cotton, P. Aylott, ‘’A simulation tool to predict the impact of soil topologies on coupling between a light rail system and buried third party infrastructure’’ , IEEE Transactions on Vehicular Technology, Vol. 57, No. 3, pages: 1404-1416, May 2008.

[10] C. Charalambous, I. Cotton, ‘‘Influence of soil structures on corrosion performance of floating DC Transit Systems’’, IET Research Journals - Electric Power Applications (formerly IEE Proceedings), Vol. 1, Issue 1, pages: 9-16, January 2007.

[11] Paul, D.; DC traction power system grounding, Industry Applications, IEEE Transactions on, Volume: 38, Issue: 3, May-June 2002, DC traction power system grounding, Pages: 818 – 824.

[12] Lee, C. -H.; Wang, H. -M.; Effects of grounding schemes on rail potential and stray currents in Taipei Rail Transit Systems, Electric Power Applications, IEE Proceedings-, Volume: 148, Issue: 2, March 2001, Pages: 148 – 154.

[13] Hill, R.J.; Cai, Y.; Case, S.H.; Irving, M.R.; Iterative techniques for the solution of complex DC-rail-traction systems including regenerative braking, Generation, Transmission and Distribution, IEE Proceedings, Volume: 143, Issue: 6, Nov. 1996, Pages: 613 – 615.

[14] J. Peter Nicholson;, ‘Correcting CIPS Surveys for Stray and Telluric Current Interference’, CORROSION 2007, March 11 - 15, 2007, Nashville, Tennessee, NACE International, ID: 07182.

[15] Brenna, M. Dolara, A. ;´Leva, S. ;´Zaninelli, D. Effects of the DC stray currents on subway tunnel structures evaluated by FEM analysis, Power and Energy Society General Meeting, 2010 IEEE, 25-29 July 2010, Minneapolis, MN.

[16] Dolara, A., Foiadelli, F., Leva, S., "Stray Current Effects Mitigation in Subway Tunnels", Power Delivery, IEEE transactions on, On page(s): 2304 - 2311 Volume: 27, Issue: 4, Oct. 2012

[17] CDEGS Software, Safe Engineering Services & Technologies Ltd Montreal, Quebec, Canada Est. 1978.

[18] C. A. Charalambous, I. Cotton, P. Aylott, N. Kokkinos, “A Holistic Stray Current Assessment of Bored Tunnel Sections of DC Transit Systems”, Accepted for Future Publication in IEEE Transactions of Power Delivery, November 2012.

[19] Dawalibi, F.P.; Ma, J.; Southey, R.D.; , "Behaviour of grounding systems in multilayer soils: a parametric analysis," Power Delivery, IEEE Transactions on , vol.9, no.1, pp.334-342, Jan 1994 doi: 10.1109/61.277704.

[20] Ogunsola, A.; Mariscotti, A.; Sandrolini, L. “Estimation of Stray Current From a DC-Electrified Railway and Impressed Potential on a Buried Pipe”, Power Delivery, IEEE Transactions on Volume: 27 , Issue: 4, Digital Object Identifier: ,October 2012 , Page(s): 2238 - 2246

[21] EN 50122-2: “Railway Applications – Fixed Installations – Electrical Safety, earthing and the return circuit – Part 2: Provisions against the effect of stray currents caused by d.c. traction systems”, October 2010.

[22] Fletcher, R.G. “Regenerative equipment for railway rolling stock” Power Engineering Journal, Volume: 5, Issue: 3, May 1991, Page(s): 105 – 114.

[23] EN-50162-2004; ‘Protection against corrosion by stray current from direct current systems’ August 2004.

[24] Charalambous, C A; Cotton, I, “Stray current control and corrosion limitation for DC mass transit systems”, Release date: 2011, Publisher: The University of Manchester. https://www.escholar.manchester.ac.uk/uk-ac-man-scw:141928).

VI. Biographies

Charalambos A. Charalambous received a Class I BEng (Hons) degree in Electrical & Electronic Engineering in 2002 and a PhD in Electrical Power Engineering in 2006 from UMIST, UK. As of 2010, he is an Assistant Professor, in the Department of Electrical and Computer Engineering, at the University of Cyprus. Prior to this appointment he was with the Electrical Energy and Power Systems Group of the School Of Electrical and Electronic Engineering at the University of Manchester. His current research interests include power induced corrosion, Ferroresonance and Risk Management Applications in Power Systems.

Ian Cotton (M’98–SM’07) an Cotton (M’98, SM’05) received a Class I BEng (Hons) degree in Electrical Engineering from the University of Sheffield in 1995 and a PhD in Electrical Engineering from UMIST in 1998. He is currently Professor of High Voltage Technology in the Electrical Energy and Power Systems Group of the School Of Electrical and Electronic Engineering at the University of Manchester. His current research interests include power systems transients, the use of higher voltage systems in aerospace applications and power system induced corrosion. He is a Chartered Engineer.

Pete Aylott received the M.A. degree (Hons.) in natural sciences from the University of Cambridge, Cambridge, U.K., in 1981. Since 1985, he has been with CAPCIS Ltd (now Intertek-CAPCIS), Manchester, U.K., where he is currently the Commercial Director. His consultancy experience covers the management of stray current on light rail and heavy rail underground systems and the interactions between these and the utility systems both across the U.K. and overseas.